

# Immobilizing a Drop of Water: Fabricating Highly Hydrophobic Surfaces that Pin Water Droplets

Adam Winkleman,<sup>†</sup> Gilad Gotesman,<sup>†</sup> Alexander Yoffe,<sup>‡</sup> and Ron Naaman<sup>\*,†</sup>

*Department of Chemical Physics, Chemical Support, Weizmann Institute of Science,  
Rehovot 76100, Israel*

*Received February 1, 2008; Revised Manuscript Received February 18, 2008*

## ABSTRACT

We describe the fabrication of a patterned, hydrophobic silicon substrate that can pin a water droplet despite its large contact angle. Arrays of nm tips in silicon were fabricated by reactive ion etching using polymer masks defined by photolithography. A droplet sitting on one class of these substrates did not fall even after the substrate was turned upside-down. The production allows the fabrication of large arrays of tips with a one-step simple etching process, along with silanization, to achieve a substrate with both very large contact and tilting angles.

Maintaining the position of a nearly spherical drop of water on a hydrophobic substrate appears to be a contradiction; typically, water droplets easily move across such surfaces and cannot be attached to a well-defined position. We describe a method for fabricating a silicon surface on which a droplet of water has both large contact and tilting angles, effectively pinning a nearly spherical drop in place.

The ability to retain a well-defined drop on a substrate may have great technological significance, including the ability to spectroscopically probe a single drop over extended periods of time. This technique could serve as an important tool in single-molecule spectroscopy, which is often limited by the short residence time of each molecule within the illuminated volume. In the past, molecules were immobilized on a substrate in order to probe minute biological material. This was done either by directly linking the probed molecule to the substrate<sup>1–6</sup> or by immobilizing the molecules by inserting them into surface-tethered lipid vesicles.<sup>7</sup> These various methods may affect their structure and/or reactivity. The present method allows, in principle, the pinning of a water drop for very long times without affecting the properties of molecules dissolved in the water.

The basic technology for fabricating arrays of silicon nm tips has been known for several decades<sup>8</sup> and has found numerous applications such as field emitter arrays in vacuum microelectronic devices (e.g., flat panel displays)<sup>9</sup> and, recently, as tips for AFM microscopy.<sup>10,11</sup> The standard method for fabricating nanotips in silicon combines photolithography and reactive ion etching (RIE) using a silicon

oxide, a silicon nitride mask, or a hydrogenated-carbon mask.<sup>9,10,12,13</sup>

Many of the methods for designing new materials that have large contact angles (greater than 150°) combine a set of common physical and chemical characteristics: (i) patterning roughness on two very different length scales (both  $\mu\text{m}$  and nm scales) and (ii) using chemical methods to present hydrophobic moieties at the surface.<sup>14–16</sup> These superhydrophobic surfaces have shown potential for applications in water-repelling substrates and self-cleaning surfaces (specifically, silicon-based solar cells).<sup>15,17,18</sup>

Large contact angles are typically associated with small tilting angles: less than 5° for superhydrophobic surfaces. Notable exceptions to this observation include pinned water droplets on a film of aligned polystyrene nanotubes,<sup>16,19,20</sup> an etched aluminum alloy composed of micro-orifices and nanoparticles,<sup>21</sup> and a monolayer of an organo- or fluorosilane self-assembled onto a laser-ablated silicon wafer.<sup>22</sup> In these systems, the water droplet could be suspended upside-down without rolling or falling from the surface. These works have led to a debate in the literature as to the definition of superhydrophobicity and possible microscopic mechanism for this macroscopic observation.<sup>23,24</sup> The suggested mechanism underlying this pinning effect is that the droplet wets the substrate, and this wetting creates a large contact area between the droplet and the surface. Because of the high surface roughness of the substrate, the sum total of the van der Waals forces between the droplet and the substrate integrated over this large contact area is sufficient to pin the drop onto the surface. Another hypothesis is that a placed drop on the surface creates pockets of air isolated from the atmosphere and this trapped air increases the adhesion

\* Corresponding author. E-mail: ron.naaman@weizmann.ac.il.

<sup>†</sup> Department of Chemical Physics, Weizmann Institute of Science.

<sup>‡</sup> Chemical Support, Weizmann Institute of Science.

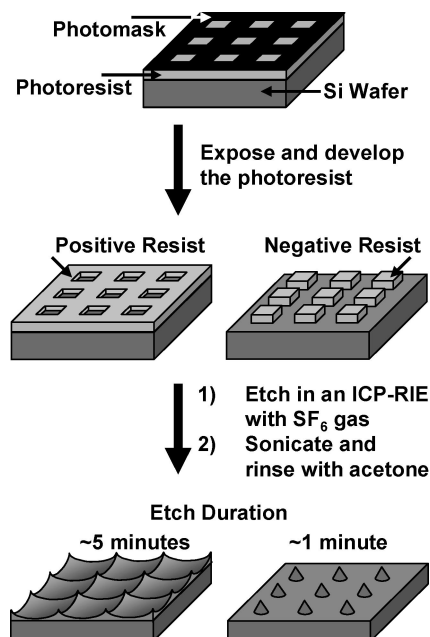


**Figure 1.** Schematic drawing illustrating the main steps in the fabrication of nm tips in silicon. We spun-cast a 1–2  $\mu\text{m}$  thick film of either a positive or negative photoresist onto a flat silicon wafer. The photomask consisted of a grid of crossed lines 2.5  $\mu\text{m}$  wide, spaced by 2.5  $\mu\text{m}$  in both directions. After exposure and development of the photoresist, the substrates were placed in an ICP-RIE and etched by  $\text{SF}_6$  gas, using the photoresist as the etch mask. The substrates with the positive resist mask were etched for  $\sim 5$  min, and the negative resist was etched for  $\sim 1$  min. Upon completion of the etching process, the substrates were sonicated and washed with acetone and isopropyl alcohol to remove the photoresist. Last, we silanized the substrates to create hydrophobic surfaces.

because of a negative pressure induced by the increase in volume of an air pocket as the drop is pulled away from the surface.<sup>21,24</sup> These mechanisms are similar to the one proposed to explain the capabilities of a gecko's feet.<sup>25</sup>

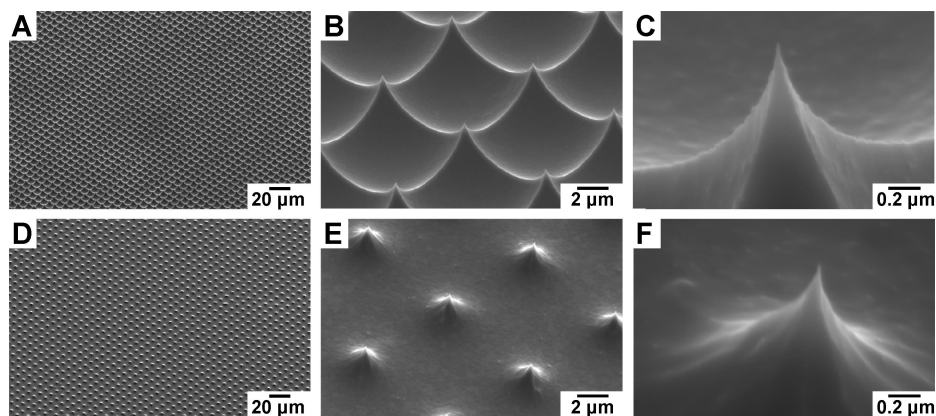
In this letter, we report the fabrication of arrays of nm tips in silicon using both positive and negative photoresist as the mask for creating surfaces by inductively coupled plasma reactive ion etching (ICP-RIE), with features ranging in size from nanometers to micrometers. These tips were fabricated with features over 2 orders of magnitude, where the smallest features, the diameter of the tip, were as small as 15 nm. Upon silanization of these surfaces with hydrophobic monolayers (e.g., octadecyltrichlorosilane (OTS) or (1*H*,1*H*,2*H*,2*H*-perfluorooctyl)silane (PF)), the substrates fabricated from the positive photoresist yielded contact angles  $>140^\circ$  and as large as  $162^\circ$ . The tilting angle was defined as the angle at which the drop falls from the surface. When a water droplet was positioned on the surface and the substrate was tilted slowly, the droplet did not roll or slide even for angles up to  $90^\circ$ . For those substrates, the drop could also be flipped  $180^\circ$  and suspended upside-down.

Figure 1 outlines the procedure used to fabricate the arrays of nm tips in silicon. Either a positive or negative photoresist was spun-cast onto a silicon wafer. (For clarity and brevity, we define substrates that used a positive photoresist as positive substrates and a negative resist as negative substrates.) The photomask was a chromium mask consisting

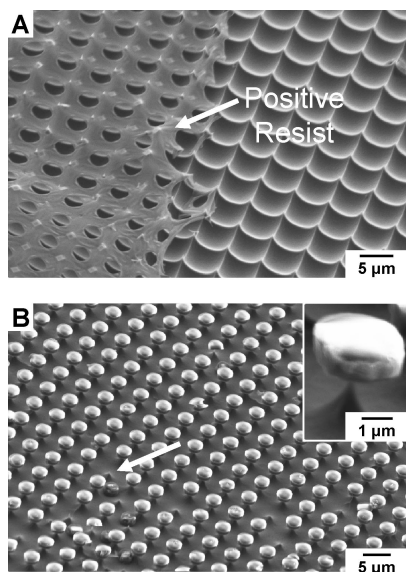
of a grid of 2.5  $\mu\text{m}$  lines spaced by 2.5  $\mu\text{m}$  in both directions. Both the positive and negative substrates were exposed through this mask, and the resists were developed to yield either an array of square wells or square posts, respectively. Unlike previously reported methods for fabricating nm tips, we use the patterned photoresist directly as the mask for the RIE procedure and not a silicon oxide or nitride layer, as is more common.<sup>9,10,12</sup> Using the photoresist as the etching mask simplifies the processing of the silicon substrate by eliminating at least one step. The main requirement for the photoresists was that they should not degrade during the RIE process. A  $\text{SF}_6$  gas/plasma (10 mT, 80 sccm, 2 kW applied to the coil) etched the silicon substrates for  $\sim 5$  and  $\sim 1$  min, respectively. Details of the experimental procedures are given in the Supporting Information. Both the positive and negative photoresists survive the RIE process, and the photoresists had to be removed by sonication in organic solvents to yield the array of nm tips.

Figure 2 shows SEM images of the nm tip arrays. Positive substrates yielded a silicon surface with lots of curvature and nm tip structures located under the vertices of the grid-patterned photoresist with additional raised features spanning the tips (Figure 2A–C). The nm tips formed were typically 15–50 nm in diameter, and the height from the tip to the nadir of the well was  $\sim 1$ –2  $\mu\text{m}$ . Conversely, the negative substrates yielded isolated nm tips on a relatively smooth silicon surface (Figure 2D–F). The range of tip diameters on the negative substrates was similar, but the height was shorter (less than 1  $\mu\text{m}$ ) than that of the positive structures. Both structures yielded highly ordered arrays over large areas exceeding 1  $\text{cm}^2$ . The major defect in both types of nm tips was due to nonuniform RIE. These defects were typically pitting in the regions between the nm tips; these features were much more common with the structures made from the positive photoresist.

Fabrication of regular nm tips, especially for those samples using a positive photoresist mask, was very sensitive to the etching times in the ICP-RIE. For example, differences of 1–2% in the etching time (i.e.,  $\sim 5$  s change for a total time of about 5 min for an etch) were often the difference between obtaining a desired sample or one that was either an underetched sample or was overetched. If the time was too short, the etching would be insufficient, resulting in an hourglass-like structure with a relatively large flat top region that was the original silicon wafer surface (Supporting Information, Figure 1A). For overetched substrates, the plasma typically etched away the nm tips and created shorter structures with nonregular angles and tunneling between adjacent nadir regions (Supporting Information, Figure 1B,C). Even for well-etched samples, we always observed some regions of pitting. These regions were typically tens to hundreds of micrometers in diameter and appeared optically as dark regions on the substrate. These “dark” features were due to nonuniform exposure to the plasma during the etching process, and they are correlated with defects in the lithography (Supporting Information, Figure 2). The nonuniformity of the lithography may result from



**Figure 2.** Set of SEM images of the nm tips surfaces illustrating length scales that span 2 orders of magnitude for both the substrates etched through the positive and negative photoresist masks. (A–C) Substrates etched through the positive photoresist mask; (D–F) substrates etched through the negative photoresist mask. The magnification in each image is the same for both sets of substrates. (A,D) In both substrates, the tips are fabricated with long-range order and uniform feature sizes. (B,E) The nm tips have the same periodicity and density; however, the exact position of the nm tips relative to the photomask is opposite for the two samples. (B) The nm tip was formed by the intersection of the crossed lines of the polymer mask. A raised edge connected each tip to one of its four neighboring tips and resulted in a nadir region in the center; these raised edges yielded a nm tip with four facets. The final structure from a substrate with a positive mask was an “egg carton” structure. (E) The etched surface between the tips is relatively smooth and flat, and the tips do not have a distinct number of facets. (C,F) An image of a single nm tip with a diameter of  $\sim 15$  nm for both substrates; this size nm tip is common but represents the smaller end of the range of tip diameters we observe.



**Figure 3.** Set of SEM images after RIE and a rinsing step but without sonication in organic solvents. These images illustrate that both the positive (A) and negative (B) photoresist masks survive intact the RIE process. In (A), the cross line pattern of the positive resist mask can clearly be observed; the resist maintains its integrity. In (B), the negative resist remains as a cap on top of the tip. In some cases, the resist fell from the tip during the processing (white arrow). The inset is a magnified image of a single tip with the negative resist still on top.

defects in the photoresist mask, which affected the local electric field and the plasma flow patterns in the ICP-RIE.

Figure 3 shows a set of SEM images of positive (3A) and negative (3B) photoresist masks that survive intact the RIE process. The cross line pattern of the positive resist mask can clearly be observed; the resist maintains its integrity, while the negative resist remains as a cap on top of the tip. In some cases, the resist fell from the tip during the processing

(white arrow). The resists charge during scanning and cause small distortion in the image.

Wet-etching processes, although more isotropic, could not produce the expected results. The positive resists are soluble in organic solutions and basic aqueous solutions, typical solvents for etching silicon wafers. The negative resist is insoluble in most solvents; however, it has poor adhesion to silicon. Lift-off of the resist from the silicon was common especially if there was any agitation (i.e., sonication or stirring) during the etching.

We also fabricated posts in silicon that have a pitch and height similar to the same masks used for making the nm tip structures (Supporting Information, Figure 3). The substrates containing posts differed from the substrates with nm tips; these differences affected the hydrophobic character of the substrates. The differences were as follows: (i) The surface roughness of the posts was more uniform across the entire  $\sim 1$  cm<sup>2</sup> sample. The use of the Bosch process created vertical side walls and prevented pitting of the etched silicon. (ii) The silicon surface of the posts was also locally less rough than the local roughness of the nm tip substrates; the top surface, which was protected from the plasma etch, was the original polished silicon.

Because these substrates possess surface roughness over multiple length scales, a property characterizing superhydrophobic materials, we measured both the contact and tilting angles of these substrates with water. All patterned silicon substrates with a native oxide surface were found to be hydrophilic, and the contact angle could not be measured because water wet the surface and penetrated between the nanotips, thus preventing a reliable measurement. Silanization of the substrates with either OTS or PF yielded hydrophobic surfaces, and for these coated samples, we were able to measure the contact angles.



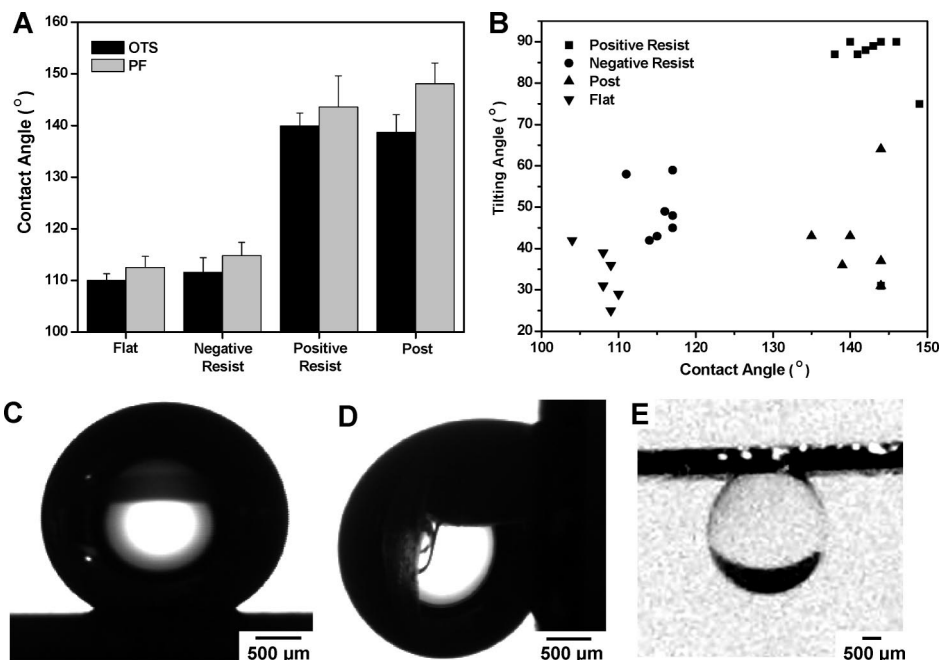


**Figure 4.** (A) The average contact angle for each of the four silicon substrates (flat silicon, nm tips from negative resists and positive resists, and posts) with both an OTS and a PF monolayer surface. (B) The contact angle of the four silicon substrates with a PF monolayer vs the tilting angle for each substrate. The substrates from the positive resist that yielded tilting angles near 90° did not roll off the substrate; the small differences in the tilt angle are from the limitations of our experimental apparatus. (C–E) Optical images of a 4  $\mu$ L drop of water on a substrate from a positive resist. (C) The contact angle for this drop is 147°. (D) Optical image of a drop of water pinned to the substrate when the tilting angle was  $\sim$ 90°; gravity deforms the drop shape, but the drop does not move along the surface. (E) Drop suspended upside-down by manually rotating the substrate 180°.

Figure 4A shows a graph of the contact angle for the four different types of substrates: flat silicon, negative substrates, positive substrates, and posts all covered with either an OTS or a PF monolayer. We used a 4  $\mu$ L drop of water for all measurements because this drop size was the minimum volume that we could successfully transfer from the needle to the substrates. The errors reported in our measurements represented the standard deviation from each set of samples; however, it should be noted that the difference between two adjacent pixels in the image analysis for the contact angle was  $\sim$ 5°. The PF-coated substrates yielded only slightly larger contact angles than OTS. The negative and positive substrates both present similar-sized nm tips with a similar pitch, but the contact angle, and thus the surface energy of these two substrates, was very different. Whereas the negative substrates had contact angles very similar to those of flat silicon, the positive substrates exhibited contact angles similar to those of the posts. The main differences between the two types of surfaces are the degree of roughness and the size of the surface features. The negative substrates are mostly smooth, between the nm tips, and the tip height is relatively short, creating a substrate similar to a flat silicon wafer. In contrast, the positive substrates and the posts are both characterized by heights larger than 1  $\mu$ m and a larger effective surface area; however, the surface roughness appears to be quite different between these substrates.

The highly pitted regions, i.e., those regions that appear darker optically and are observed predominately on the positive substrates, had higher contact angles than their surrounding area. After placing a drop of water directly over

a dark region, we typically observed the drop to initially shift away from these regions. The results reported here are the equilibrium measurements after the drops had settled on the surface. The largest variance in the contact angle was among the positive substrates due to their high sensitivity to fluctuations in the etching process. These data suggest that the predominant contribution to the large contact angle is the surface roughness and not the exact chemical nature of the hydrophobic surface. For measurements obtained from highly pitted regions, we measured contact angles as large as 162°.

We built a device consisting of our sample positioned on the axis of a spindle that was placed along the axis of the CCD camera and the light source of the contact angle goniometer. The surface was tilted by manually turning a reel above the spindle attached by a string to one end of the sample. Sometimes, upon tilting the surface, the drop did move slightly without falling. The distance of this motion was typically on the order of the diameter of the drop or less. We were careful to increase the angle as slowly and steadily as possible because the drops would fall from the surface at much lower tilting angles if the motion was either too quick or too erratic.

The tilting angle was measured on flat silicon, posts, negative, and positive substrates, all of which had a PF monolayer. The angles for the flat substrates and the posts were similar, typically from 25 to 45°. The most surprising results were for the positive substrates; usually the droplet of water did not fall off the substrates at 90°, the maximum angle that could be achieved with our measuring device.

There was one positive substrate for which the drop rolled from the surface at 31°, the same angle as for the lowest post and which was similar to the flat substrates. For those substrates whose drop remained stationary at 90°, the sample could be flipped manually to 180° and the drop remained attached to the surface. The minimum required adhesive force, per unit of planar surface area, to keep this drop attached to the substrate at 180° is  $\sim 10$  pN/mm<sup>2</sup>.

In the present case, the substrates have ordered structures, on the size scale of tens to hundreds of nanometers evenly spaced by a few micrometers plus a surface roughness of a few nanometers due to the etching process. This type of substrate is different from former cases that demonstrated both high contact angle and large tilting angles. The features in the aluminum alloy substrate by Guo and Liu are larger than our features on both scales and lack very small dimensions as micro-orifices on the scale of 10–30  $\mu$ m and nanoparticles 80–100 nm.<sup>21</sup> The array of PS nanotubes by Jin et al. was highly ordered like our features; however, the density of nanotubes is about 2 orders of magnitude greater than our tips and lacks features with lateral dimensions on the micrometer scale.<sup>19</sup> Also the chemical nature of these three systems vary greatly, including a semiconductor (fluorinated silicon), a metal (untreated aluminum alloy), and a dielectric (polystyrene). The common feature of all systems in which pinning of water drops is observed, together with high contact angle, is the presence of regions with pores that could possibly trap air that is isolated from the atmosphere. It seems that the small degree of pitting, described above, is crucial to the adhesion. This pitting is not observed in overetched substrates, where the pitting would be interconnected to the atmosphere, or in underetching, where no pits are present.

In conclusion, this letter describes the fabrication of large arrays of nm tips with a one-step simple etching process, together with silanization, to achieve a substrate with both very large contact and tilting angles. The advantages of this process are as follows: (i) it uses standard chemical processes (photolithography, RIE, and silanization) and materials (silicon wafers), (ii) it makes surfaces over relatively large areas ( $> 1$  cm<sup>2</sup>), and (iii) it yields very hydrophobic surfaces that allow for ease of handling of substrates after applying a water drop without loss of the drop. The drawbacks of these substrates are that a clean room facility is required for fabrication, the exact nature and features of the surface are very sensitive, and much care must be taken to achieve reproducibility.

We believe that the discovery of new materials that broaden the definition of superhydrophobicity will help to determine and clarify the microscopic mechanism for this macroscopic observation and will open the way for new applications.

**Acknowledgment.** This work was partially supported by the Grand Center and by the Israeli Ministry of Science.

**Supporting Information Available:** Experimental procedures. This material is available free of charge via the Internet at <http://pubs.acs.org>.

## References

- (1) Ha, T.; Glass, J.; Enderle, T.; Chemla, D. S.; Weiss, S. *Phys. Rev. Lett.* **1998**, *80*, 2093.
- (2) Wazawa, T.; Ishii, Y.; Funatsu, T.; Yanagida, T. *Biophys. J.* **2000**, *78*, 1561.
- (3) Jia, Y.; Talaga, D. S.; Lau, W. L.; Lu, H. S. M.; DeGrado, W. F.; Hochstrasser, R. M. *Chem. Phys.* **1999**, *247*, 69.
- (4) Noji, H.; Yasuda, R.; Yoshida, M.; Kinoshita, K. *Nature* **1997**, *386*, 299.
- (5) Wennmalm, S.; Edman, L.; Rigler, R. *Proc. Natl. Acad. Sci. U.S.A.* **1997**, *94*, 10641.
- (6) Ha, T.; Zhuang, X.; Kim, H. D.; Orr, J. W.; Williamson, J. R.; Chu, S. *Proc. Natl. Acad. Sci. U.S.A.* **1999**, *96*, 9077.
- (7) Boukobza, E.; Sonnenfeld, A.; Haran, G. *J. Phys. Chem. B* **2001**, *105*, 12165.
- (8) Thomas, R. N.; Nathanson, H. C. *Appl. Phys. Lett.* **1972**, *21*, 384.
- (9) Temple, D. *Mater. Sci. Eng. R* **1999**, *24*, 185.
- (10) Wang, Y. Q.; van der Weide, D. W. *J. Vac. Sci. Technol., B* **2005**, *23*, 1582.
- (11) Knapp, H. F.; Stemmer, A. *Surf. Interface Anal.* **1999**, *27*, 324.
- (12) Alves, M. A. R.; Takeuti, D. F.; Braga, E. S. *Microelectron. J.* **2005**, *36*, 51.
- (13) Takeuti, D. F.; Tirolli, M. N.; Danieli, C. L.; Alves, M. A. R.; Braga, E. S.; de Faria, P. H. L. *Microelectron. J.* **2007**, *38*, 31.
- (14) Ma, M. L.; Hill, R. M. *Curr. Opin. Colloid Interface Sci.* **2006**, *11*, 193.
- (15) Zhang, X.; Shi, F.; Niu, J.; Jiang, Y.; Wang, Z. Q. *J. Mater. Chem.* **2008**, submitted for publication.
- (16) Li, X. M.; Reinhoudt, D.; Crego-Calama, M. *Chem. Soc. Rev.* **2007**, *36*, 1350.
- (17) Prevo, B. G.; Hon, E. W.; Velev, O. D. *J. Mater. Chem.* **2007**, *17*, 791.
- (18) Furstner, R.; Barthlott, W.; Neinhuis, C.; Walzel, P. *Langmuir* **2005**, *21*, 956.
- (19) Jin, M. H.; Feng, X. J.; Feng, L.; Sun, T. L.; Zhai, J.; Li, T. J.; Jiang, L. *Adv. Mater.* **2005**, *17*, 1977.
- (20) Hong, X.; Gao, X. F.; Jiang, L. *J. Am. Chem. Soc.* **2007**, *129*, 1478.
- (21) Guo, Z.-G.; Liu, W.-M. *Appl. Phys. Lett.* **2007**, *90*, 223111.
- (22) Song, X. Y.; Zhai, J.; Wang, Y. L.; Jiang, L. *J. Phys. Chem. B* **2005**, *109*, 4048.
- (23) Li, W.; Amirfazli, A. *Adv. Mater.* **2007**, *19*, 3421.
- (24) Wang, S.; Jiang, L. *Adv. Mater.* **2007**, *19*, 3423.
- (25) Autumn, K.; Liang, Y. A.; Hsieh, S. T.; Zesch, W.; Chan, W. P.; Kenny, T. W.; Fearing, R.; Full, R. J. *Nature* **2000**, *405*, 681.

NL080317D